JAPANESE JOURNAL OF APPLIED PHYSICS
VOL. 30, NO. 7, JULY, 1991, pp. 1400–1404

Operating Characteristics of Optically Addressed Spatial Light Modulators Incorporating Distorted Helix Ferroelectric Liquid Crystals

Bruce LANDRETH, Chong-Chang MAO and Garret MODDEL

Department of Electrical and Computer Engineering and Center for Optoelectronic Computing Systems, University of Colorado, Boulder, Colorado, 80309-0425, USA

(Received December 31, 1990; accepted for publication April 20, 1991)

Distorted helix ferroelectric liquid crystals have received attention recently due to the availability of short-pitch, high-spontaneous-polarization mixtures. In this paper we discuss the operating characteristics of an optically addressed spatial light modulator incorporating a hydrogenated amorphous silicon photosensor and a distorted-helix ferroelectric liquid crystal light modulator. The device exhibits a grey-scale response over a range of write-light intensities which depends on operating frequency. The spatial resolution is 30 lp/mm. The time-averaged contrast ratio is 7:1, limited primarily by non-uniformity in the liquid crystal alignment. During switching, both the average optic axis orientation and the effective birefringence of the liquid crystal change. The capability of the device to produce a pseudocolored readout image is attributed to the latter effect.

KEYWORDS: amorphous silicon, distorted helix, ferroelectric liquid crystal, pseudocolor, spatial light modulator

Optically addressed spatial light modulators (OASLMs) are devices which provide a means for the interaction of two light beams. In the most common case, a write-light beam is incident upon a photosensor which generates a control signal for the read-light modulator. In contrast to most electronically-addressed spatial light modulators, the entire active area of an OASLM can be updated simultaneously. Early development efforts were motivated by wavelength conversion and projection display[1] applications. More recently, interest in optical processing has generated new applications for OASLMs, including input transducers, processing elements and storage devices. There are many OASLMs currently under research and development.[2] All provide for both detection and modulation of light.

Several OASLMs using liquid crystal light-modulating layers have been reported. The majority of these devices incorporate either nematic liquid crystals (NLCs) or surface-stabilized ferroelectric liquid crystals (SSFLCs). NLCs have an inherently analog optical response to applied voltage, and hence to incident write-light intensity in OASLMs. SSFLCs, on the other hand, have an inherently binary response to applied voltage.[3] However, the time required to switch SSFLCs between the two stable states is voltage-dependent.[4] In OASLMs, the liquid crystal voltage is controlled by the photosensor, and hence the switching speed increases with write-light intensity. Therefore, an analog optical response can be obtained by electrically cycling the device on and off fast enough that the SSFLC switching transient dominates the intensity transfer characteristic.[5]

Other liquid crystal light modulation effects used in OASLMs include the electroclinic effect in smectic A* liquid crystals,[6,7] and the distorted helix ferroelectric effect in smectic C* liquid crystals.[8] Both provide modulation which changes continuously with applied voltage. An OASLM using the electroclinic effect which exhibited microsecond response times was reported recently.[9] These devices must be operated at constant temperature because the intensity transfer characteristic is strongly temperature-sensitive, particularly near the smectic A* to smectic C* transition temperature where the read-light modulation is largest.

Distorted helix ferroelectric liquid crystals (DHFLCs) have become more attractive for light-modulation applications recently because of the availability of short-pitch, high-polarization mixtures.[10,11] Light propagating through these materials perpendicular to the helix axis responds to a spatially-averaged optic axis and birefringence. Distortion of the helicoidal structure by applied voltages changes both of these parameters. As the helix distorts, the pitch increases until the unwinding voltage is reached, at which point the helix is effectively unwound and a uniform structure results. In this state, the DHFLC structure is similar to that of an ideal SSFLC in one of its two stable orientations. Under applied voltages of either polarity which are less than the unwinding voltage, continuous rotation of the average optic axis between the two opposite-sense unwound endpoints is possible. A DHFLC OASLM was described briefly by Beresnev *et al.*,[12] and the color-modulating capabilities of DHFLCs were analyzed in a recent paper by Abdulhalim and Moddel.[13] In the present paper, we discuss the operating characteristics of an OASLM incorporating a hydrogenated amorphous silicon (a-Si:H) photosensor and a short-pitch, high-polarization DHFLC light modulator.

Figure 1 shows the structure of our OASLMs. The a-Si:H photosensor is a p-i-n photodiode which has been described elsewhere.[14] The liquid crystal is Hoffman LaRoche mixture FLC-6200. This material exhibits a chiral smectic C (SmC*) phase between −3 and 59°C, and a room-temperature helicoidal pitch of 0.37 μm and tilt angle of 27°. The cells were filled under vacuum by capillary action in the isotropic phase. The nominal thickness of the DHFLC layer is 2.4 μm, set with glass-rod spacers. This thickness was chosen to make the cell a second-order reflection-mode half-wave plate. Rubbed

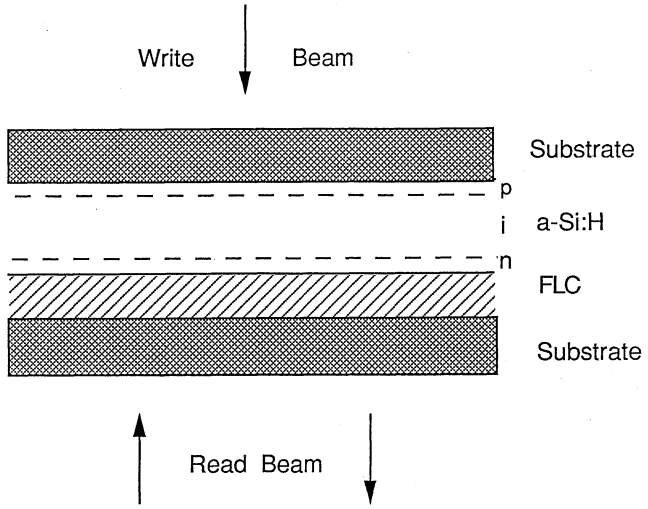

Fig. 1. Cross-section of the OASLM showing the a-Si:H photodiode and the FLC light-modulating layer.

polymeric layers on both substrates induced homogeneous alignment during cooling. The active area of the device is 12 mm in diameter.

The existence of a helicoidal structure was verified by illuminating the devices with collimated 633 nm laser light and observing the diffraction pattern which results from the periodicity of the helix. Four reference cells without photosensors having FLC thicknesses of 1, 2, 3 and 5 μm were also studied. Under zero applied voltage, only a weak diffraction pattern was obtained from the 1 μm cell, indicating that a well-defined helix was not present. The strength of the diffraction pattern increased with cell thickness. The diffraction patterns became weaker as increasing dc voltage of either polarity was applied, consistent with the distortion and unwinding of the helix. The voltage at which the diffraction pattern was no longer visible was taken as the unwinding voltage. To determine appropriate operating conditions, bipolar square voltage waveforms of varying amplitude and frequency were applied to the OASLMs while observing the time-averaged diffraction pattern. A high-intensity write-light was applied during these tests to prevent rectification of the applied voltage waveform by the a-Si:H photodiode. The unwinding voltage amplitude increased from 2.5 volts at 50 Hz to 10 volts at 2 kHz. To obtain the unique light modulation effects associated with the winding and unwinding of the helix, an operating voltage amplitude less than the unwinding voltage was used during OASLM operation.[15]

The spatial and temporal responses of the OASLMs were measured in a standard reflection-mode test system.[14] The write-light laser had a wavelength of 514 nm, while the read-light wavelength was 633 nm. Both beams were spatially filtered and collimated. To operate the device, a square-wave voltage was applied between the two transparent conducting oxide electrodes. The frequency of this applied waveform is referred to as the device operating frequency. When the voltage is positive, the photodiode is forward-biased, the applied voltage drops across the liquid crystal, and the device is erased. The OASLM was oriented between crossed polarizers to obtain the minimum readout intensity at the end of this period. When the applied voltage becomes negative, the diode is reverse-biased and the liquid crystal is charged up to the applied voltage at a rate which is proportional to the write-light intensity. Although the write-light was on continuously during these experiments, it had an effect on the read-light modulation only during the reverse-biased write period.

The vertically-polarized incident read beam propagated through the FLC layer and was partially reflected from the FLC/a-Si:H interface. This reflected component was then analyzed by a horizontally oriented polarizer and focused by an output lens. Time-resolved responses to uniform write-light distributions were measured with a single-element photodiode centered in the back focal plane of the output lens, while spatially resolved responses to write-light images were observed with a CCD video camera placed in the image plane. The time-averaged diffraction efficiency resulting from interferometrically generated, spatially sinusoidal write-light inputs was measured by placing the CCD camera in the back focal plane of the output lens.

Figure 2 shows the transient response of a DHFLC OASLM for six different uniform write-light intensities. In this figure, the reverse-biased write period occurs between 0 and 1 ms, and the forward-biased erase period occurs between 1 and 2 ms. The amplitude of the applied bipolar square wave was 5 volts, chosen so that the device operated within the range of continuous helix distortion, as determined from the diffraction-pattern observations. As with SSFLC OASLMs, a grey-scale response results from the inverse dependence of the liquid crystal rise time on write-light intensity.[5] The relationship between the rise time and the write-light intensity can be measured accurately over a wide range by varying the device operating frequency. At low frequencies, the write period is longer and hence lower write-light intensity is re-

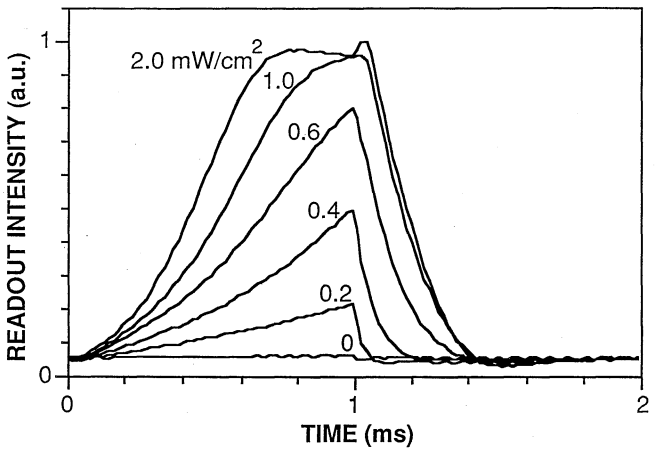

Fig. 2. Digital oscilloscope traces showing the transient readout response of an OASLM having a DHFLC thickness of 2.4 μm. The data were obtained at an operating frequency of 500 Hz for write-light intensities of 0, 0.2, 0.4, 0.6, 1 and 2 mW/cm^2, as noted in the figure. Although the write-light is on continuously in these tests, it affects read-light modulation only during the period between 0 and 1 ms, when the photodiode is reverse-biased.

quired to switch the liquid crystal fully on within the write period. From such experiments we found that the 10–90% DHFLC rise time varies from 20 ms at a write-light intensity of 10 μW/cm^2 to 200 μs at a write-light intensity of 5 mW/cm^2.

The change in light output during the DHFLC switching transient is due to both rotation of the average optic axis and birefringence change. An analytical expression for reflection-mode light modulation by an optically-uniaxial material between crossed polarizers is

$$I_r = \sin^2(2\theta)\sin^2(2\pi\Delta nd/\lambda) \quad (1)$$

where I_r is proportional to the reflected read-light intensity which passes through the analyzer, θ is the angle between the optic axis and the polarization of the incident light, Δn is the birefringence, d is the thickness and λ is the wavelength of light. In the absence of a change in birefringence, the readout intensity should be linearly proportional to $\sin^2(2\theta)$. The average optic axis orientation at any point along the transient can be determined by rotating the OASLM to shift the minimum in readout intensity from the end of the erase period to the point of interest. The OASLM is oriented initially with the average optic axis parallel to the polarization of the incident read-light at the end of the erase period. Therefore, the amount of rotation required to shift the minimum in readout intensity to any other point in time on the transient is equal to the angle θ in eq. (1). Figure 3 shows the result of such an experiment, plotting the initial readout intensity (prior to OASLM rotation) as a function of $\sin^2(2\theta)$ for both the turn-on and turn-off transients. The deviation from linearity on this plot is attributed to a change of birefringence during DHFLC switching. The non-coincidence of two curves on this plot shows that more than one value of birefringence is possible for a given optic axis orientation. We believe this effect is responsible for the local maximum in readout intensity which occurs during the first 200 μs of erase periods which follow write periods of high write-light intensity seen in Fig. 2. When this same test is repeated on SSFLC OASLMs, we observe a linear relation between I_r and $\sin^2(2\theta)$.

The specific form of the intensity transfer characteristic depends not only on the OASLM operating conditions but also on the method of readout. The simplest case is that of asynchronous operation, where neither the write nor read light is synchronized with the operating voltage waveform. In order to observe a stable output in this mode of operation, the read-light integration time should be long compared with the operating period of the device. This would be the case, for example, when the output of an OASLM operating at 500 Hz is observed with a 30 Hz frame rate video camera. The appropriate time-averaged intensity transfer characteristic for this mode of operation can be obtained by integrating transient responses such as those shown in Fig. 2 over one operating period. The results of this integration are shown in Fig. 4. The general form of the intensity transfer characteristic is that of a saturating nonlinearity and is similar to that observed with SSFLC OASLMS.[5] There is a range of write-light intensities over which a grey scale response is observed, followed by saturation. The width of the range of write-light intensities over which grey scale response is obtained can be increased by increasing the operating frequency of the device. Because of the dependence of rise time on write-light intensity, higher write-light intensities are required to obtain the same level of read-light output in a shorter write period.

A maximum contrast ratio of 7:1 can be calculated from the data in Fig. 4. Two mechanisms limit the contrast in these OASLMs. The most significant is nonuniformity in the liquid crystal alignment, which results in varying degrees of read beam extinction over the device aperture. The result in Fig. 2 is typical of the DHFLC cells we have made to date; in general we find that it is more difficult to obtain uniform alignment in distorted helix cells than in surface-stabilized cells. The second contribution is due to unwanted liquid crystal modulation during the write period which occurs even in the absence of write-light. This is due to capacitive coupling[14] of the operating voltage to the DHFLC. The relatively high spontaneous polarization of this mixture (100

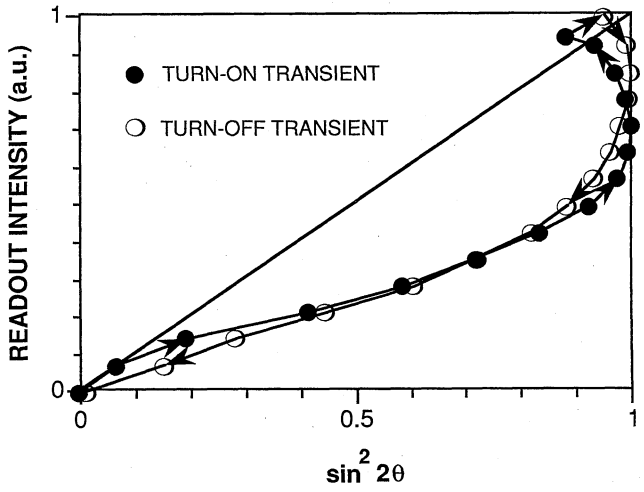

Fig. 3. Readout intensity versus $\sin^2(2\theta)$ for the 2 mW/cm^2 transient of Fig. 2. As discussed in the text, the deviation from linearity is attributed to a change in the effective birefringence during switching.

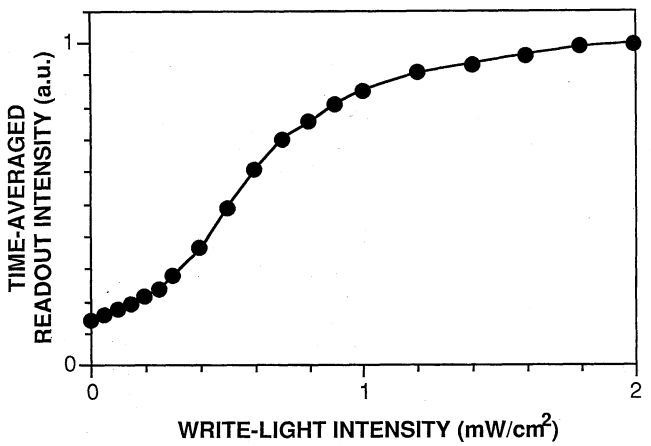

Fig. 4. Time-averaged nonlinear intensity transfer characteristic obtained at an operating frequency of 500 Hz showing the range of grey-scale operation under monochromatic read-light.

nC/cm^2) makes this contribution to contrast ratio degradation relatively small because of the large effective capacitance of the liquid crystal relative to that of the a-Si:H photodiode.

The OASLM resolution was measured by two methods: by imaging a United States Air Force resolution chart (USAF-1951) onto the a-Si:H photosensor and by calculating the modulation transfer function (MTF) from diffraction efficiency measurements. In both cases, the resolution was found to be approximately 30 lp/mm. A photograph of the readout image displayed on a video monitor is shown in Fig. 5. In the diffraction efficiency measurements, the MTF showed the expected rolloff with increasing spatial frequency, passing through 0.5 at approximately 30 lp/mm. In both cases, the optimum resolution was obtained when the write-light intensity was within the grey-scale range, driving the device into saturation decreases its resolution.

The change in birefringence during switching, as deduced from Fig. 3, can be used to produce pseudocolored readout images. To observe this effect, a white (tungsten filament) read-light and a color CCD video camera were used. In this device, the input image grey scale is mapped to a range of colors between blue and yellow. An example of this is shown in Figs. 6(a) and 6(b). The input image was the negative slide used to produce the positive print shown in Fig. 6(a). The colored image in Fig. 6(b) is a photograph of the OASLM output taken from a color video monitor. The darkest areas of the input transparency produce no output, areas of medium density produce a blue output color, and the lightest areas produce a yellow output color. Under spatially uniform write-light of increasing intensity, we first observe a continuously brighter blue read-light, followed by a rather abrupt transition to yellow. The yellow color is believed to be the color associated with the birefringence of the unwound state and the thickness of this particular cell. The green color appearing in the transition between the blue and yellow areas may be the result of temporal averaging, since the OASLM was operating at 500 Hz, the video camera at 30 Hz, and the film exposed for 2 seconds.

In summary, we have characterized the operation of an optically-addressed spatial light modulator incorporating an amorphous silicon photosensor and a distorted helix ferroelectric liquid crystal. Although the monochromatic read-light intensity transfer characteristic is functionally similar to that obtained with SSFLC OASLMs, there is a significant contribution from birefringence change as well as from optic axis rotation in the case of the DHFLC. This birefringence change can be used to obtain a pseudocolored readout image when a white read-light is used. The resolution and contrast ratio are lower than we

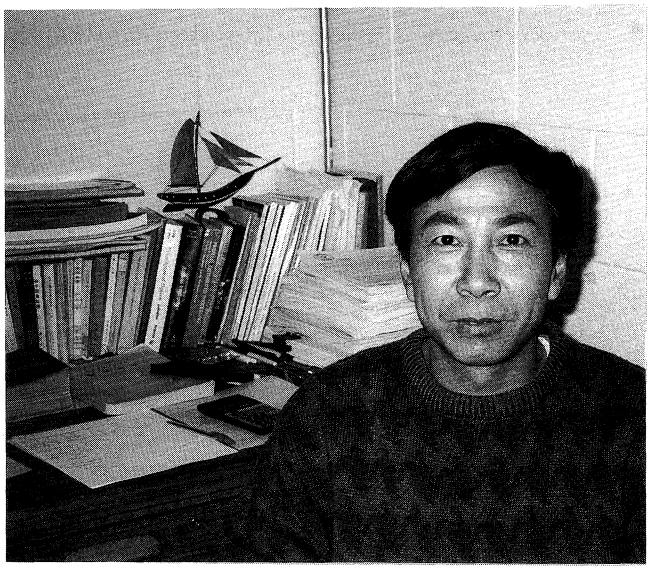

Fig. 6(a). Photograph of second author. Light transmitted through the negative transparency used to make this positive print was imaged onto the OASLM photosensor.

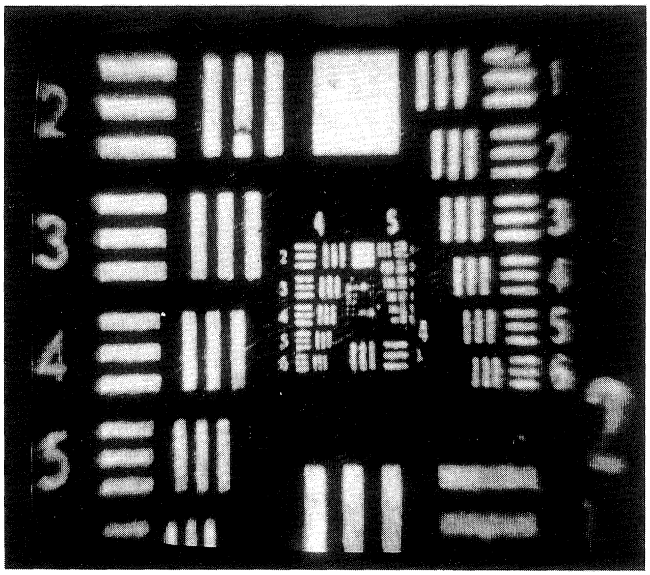

Fig. 5. Reflected read-light image response to USAF resolution chart write-light input image. The smallest resolvable pattern corresponds to a resolution of 28 lp/mm.

Fig. 6(b). Pseudocolored output image resulting from the input of Fig. 6(a). Dark areas of the input transparency result in no output, medium density areas result in blue output, and light areas create yellow output. As discussed in the text, the green intermediate color may be due to temporal averaging.

usually obtain with SSFLC OASLMs. Both of these problems can be attributed to non-uniform liquid crystal alignment.

We are grateful to J. Funfschilling of Hoffman LaRoche for providing us with the mixture FLC-6200 which was used in these OASLMs, and to D. Doroski and S. Wichart for cell fabrication. We also thank K. Johnson and I. Abdulhalim for helpful suggestions and P. Barbier, A. Gabor, R. Rice, and C. Walker for a careful review of the manuscript. This work was supported by NSF Engineering Research Center grant No. CDR-862236 and by Martin Marietta under contract number NH9-080-453.

References

1) T. D. Beard, W. P. Bleha and S. Y. Wong: Appl. Phys. Lett. **22** (1973) 90.
2) For a review, see A. D. Fisher: Int. J. Optoelectron. **5** (1990) 125.
3) N. A. Clark and S. T. Lagerwall: Appl. Phys. Lett. **36** (1980) 899.
4) X. J.-Zhi, M. A. Handschy and N. A. Clark: Ferroelectrics **73** (1987) 305.
5) B. Landreth and G. Moddel: Proc. SPIE **1296** (1990) 64.
6) S. Garoff and R. B. Meyer: Phys. Rev. Lett. **38** (1977) 848.
7) S. Garoff and R. B. Meyer: Phys. Rev. A **19** (1979) 338.
8) B. I. Ostrovskii and V. G. Chigrinov: Sov. Phys.-Crystallogr. **25** (1980) 322.
9) I. Abdulhalim, G. Moddel and K. M. Johnson: Appl. Phys. Lett. **55** (1989) 1603.
10) J. Funfschilling and M. Schadt: J. Appl. Phys. **66** (1989) 3877.
11) K. Yoshino, S. Kishio, M. Ozaki, T. Sakurai, N. Mikami, R. Higuchi and M. Honma: Jpn. J. Appl. Phys. **25** (1986) L416.
12) L. A. Beresnev, L. M. Blinov and D. I. Dergachev: Ferroelectrics **85** (1988) 173.
13) I. Abdulhalim and G. Moddel: Mol. Cryst. & Liq. Cryst. **200** (1991) 79.
14) W. Li, R. A. Rice, G. Moddel, L. A. Pagano-Stauffer and M. A. Handschy: IEEE Trans. Electron Devices **36** (1989) 2959.
15) S. S. Bawa, A. M. Biradar and S. Chandra: Jpn. J. Appl. Phys. **26** (1987) 189.